



A Cretaceous age for an alkali dolerite dyke near Smithton, NW Tasmania

Author: J. L. Everard, H. Zwingmann,
D. McP. Duncan and R. S. Bottrill
Date: 13/04/2023
Email: info@mrt.tas.gov.au
Website: www.mrt.tas.gov.au

REPORT No.: TR36



Geological Survey
Technical Report 36





Mineral Resources Tasmania
Department of State Growth

Geological Survey Technical Report 36:

A Cretaceous age for an alkali dolerite dyke near Smithton, NW Tasmania

by J. L. Everard, H. Zwingmann, D. McP. Duncan and R. S. Bottrill

Cover: Dolerite dyke in dolomite quarry, Smithton (Photo - R. S. Bottrill).

While every care has been taken in the preparation of this report, no warranty is given as to the correctness of the information and no liability is accepted for any statement or opinion or for any error or omission. No reader should act or fail to act on the basis of any material contained herein. Readers should consult professional advisers. As a result the Crown in Right of the State of Tasmania and its employees, contractors and agents expressly disclaim all and any liability (including all liability from or attributable to any negligent or wrongful act or omission) to any persons whatsoever in respect of anything done or omitted to be done by any such person in reliance whether in whole or in part upon any of the material in this report. Crown Copyright reserved.

Abstract

An ^{40}Ar - ^{39}Ar total gas age of 95.93 ± 7.37 Ma (mid-Cretaceous, possibly Cenomanian) was obtained from one of several narrow dykes of alkali dolerite exposed in a quarry at Smithton, northwest Tasmania. Aeromagnetic imagery suggests that the dykes are rare exposures of a small WNW-ESE-trending swarm. The dolerite is petrologically unlike any other known mid-Cretaceous igneous rocks in Tasmania, but is compositionally very similar to some Cainozoic basalts, and was probably produced by earlier partial melting of similar mantle sources. The orientation of the dykes was probably controlled by NNE/SSW-directed extension during the initial stages of the development of Bass Basin, approximately coeval with the commencement of rifting between Australia and Antarctica.

A Cretaceous age for an alkali dolerite dyke near Smithton, NW Tasmania

by J. L. Everard¹, H. Zwingmann², D. McP. Duncan³ and R. S. Bottrill¹

¹*Geological Survey Branch - Mineral Resources Tasmania*

²*CSIRO Division of Petroleum Resources & Centre of Excellence in Mass Spectrometry, School of Applied Geology, Curtin University, WA, (present address: Division of Earth and Planetary Science, Kyoto University, Japan)*

³*D. McP. Duncan- MRT (retired) 18 Old Summerleas Road, Kingston 7050*

CONTENTS

1.0 INTRODUCTION	4
2.0 FIELD RELATIONS	4
3.0 PETROGRAPHY	8
4.0 MINERAL CHEMISTRY	8
5.0 GEOCHEMISTRY	11
6.0 GEOCHRONOLOGY	12
7.0 DISCUSSION AND CONCLUSION	12
7.0 ACKNOWLEDGEMENTS	15
8.0 REFERENCES	16

FIGURES

Figure 1. Total magnetic intensity (TMI) image of far northwest Tasmania	4
Figure 2. Generalised geology of far northwest Tasmania, derived from MRT 1:250,000 digital data.	5
Figure 3. Detailed geology in vicinity of dolomite quarry, Smithton	6
Figure 4. Dolerite dykes in dolomite quarry, Smithton, in 2001	7
Figure 5. Dolerite dykes in dolomite quarry, Smithton, in 2006	7
Figure 6. Detail of dolerite dykes in dolomite quarry, Smithton, in 2014	8
Figure 7. Photomicrograph of alkali dolerite sample R011141D, dolomite quarry, Smithton	9
Figure 8. Photomicrograph of alkali dolerite sample R011141D, dolomite quarry, Smithton	10
Figure 9. Plots of selected major elements for Smithton alkali dolerite (R011141D)	11
Figure 10. Plots of compatible trace elements for Smithton alkali dolerite (R011141D)	12
Figure 11. Chondrite-normalised rare-earth element plot of Smithton alkali dolerite	13
Figure 12. Incompatible element spider diagram for Smithton alkali dolerite	13
Figure 13. ³⁹ Ar-age degassing spectrum.	14
Figure 14. Inverse isochron, ³⁶ Ar/ ⁴⁰ Ar vs ³⁹ Ar/ ⁴⁰ Ar	14

APPENDICES

APPENDIX 1	18
APPENDIX 2	22

1.0 INTRODUCTION

Aeromagnetic imagery of far northwest Tasmania shows a series of parallel, WNW-ESE-trending linear magnetic anomalies, most prominent between Smithton and Montagu, but possibly extending ESE to the vicinity of Mengha, and WNW toward Cape Grim (Figure 1). Although outcrop in the region is poor, the anomalies lie within areas of Mesoproterozoic (Rocky Cape Group), Neoproterozoic (Togari Group) and Late Cambrian (Scopus Formation) basement. They also cross-cut, without apparent deflection, several major structures such as the Roger River Fault (Figure 2). Therefore the age of their source or sources is clearly post-Cambrian.

Duncan (2002) noted that one of the anomalies is coincident with several narrow dykes of alkali dolerite which intrude the Smithton Dolomite, exposed in a quarry near Smithton (Figure 3). He therefore attributed the anomalies to a dyke swarm, and suggested that age dating should be attempted on the relatively fresh dolerite exposed in the quarry. Although briefly reported by Bottrill et al. (2014), the main purpose of this report is to fully document the results of that work.

2.0 FIELD RELATIONS

Duncan (2002) reported three subvertical basic dykes, up to 3m wide and trending $\sim 120^\circ$ intruding dolostone (Smithton Dolomite) on the west wall of the upper benches of the Circular Head Dolomite quarry, about 2.3 km west of Smithton (Figure 4, 5, 6). The dolostone in the quarry is recorded dipping west or WNW at 32° to 47° (i.e. approximately orthogonal to the dykes) (Lennox et al., 1982; Seymour 2001) and may be on the southwest limb of an open anticline trending $\sim 135^\circ$ (Duncan 2002). A sample (R011141) was collected from a small dyke, exposed on the floor of the pit near the east wall, which was considered to be the freshest.

About 13 km further west, where two similar subparallel WNW-trending magnetic anomalies cross Barcoo Road, auger sampling by Geopeko Ltd found anomalous levels of Pb, Fe, Ni and Ba, and “erratic” Cr values in soil samples. Although no rock chips were collected, “basic dykes” within Cambrian sedimentary rocks (now known as the Scopus Formation) were suggested as the likely source of the magnetic and geochemical anomalies, termed DB1 and DB2 (Figures 1 and 2) (Pemberton, 1983).

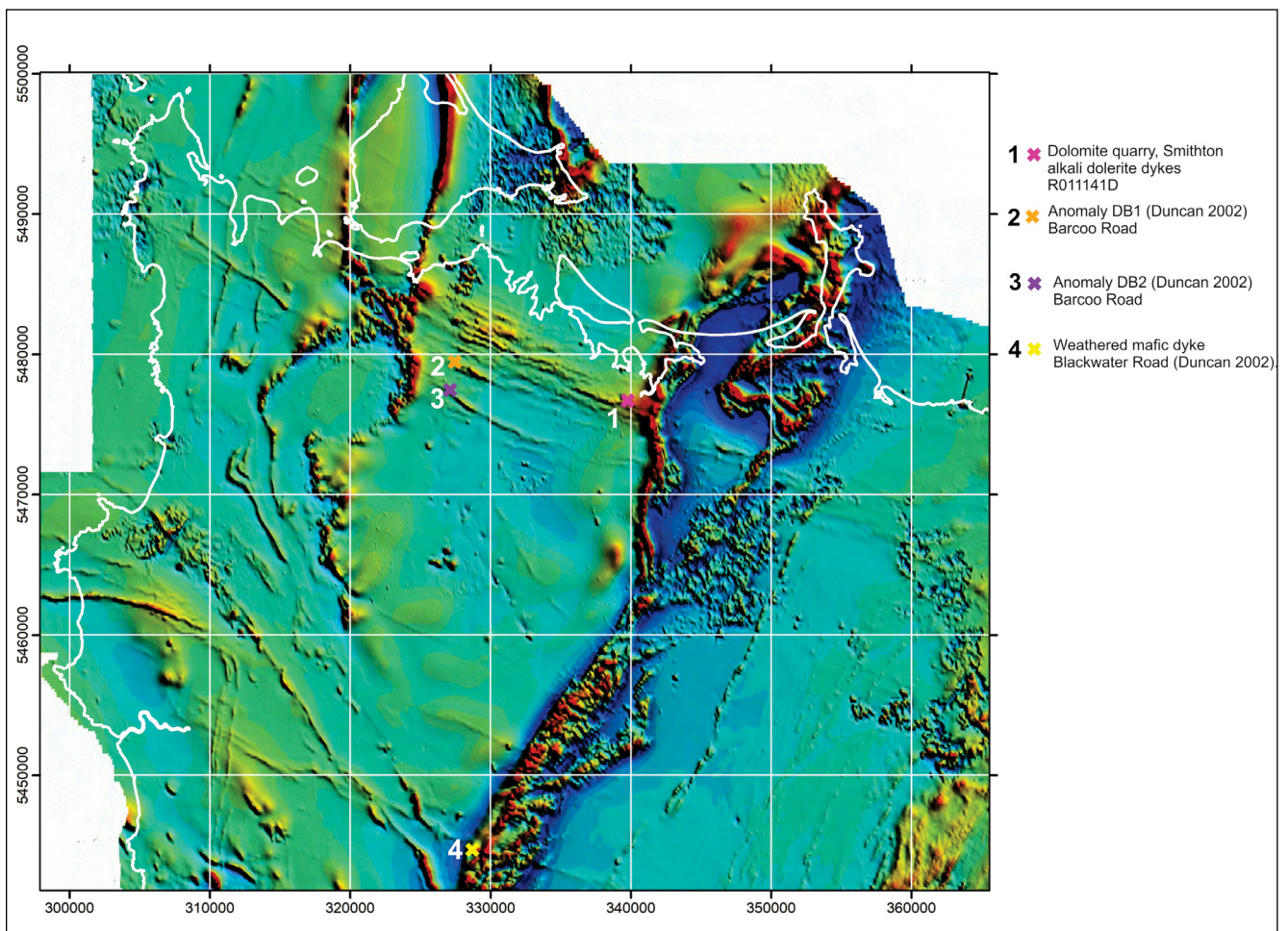


Figure 1. Total magnetic intensity (TMI) image of far northwest Tasmania, with northeast sun angle. Derived from 2001 Northwest Tasmania WTRMP Area B airborne survey, 200 m line spacing.

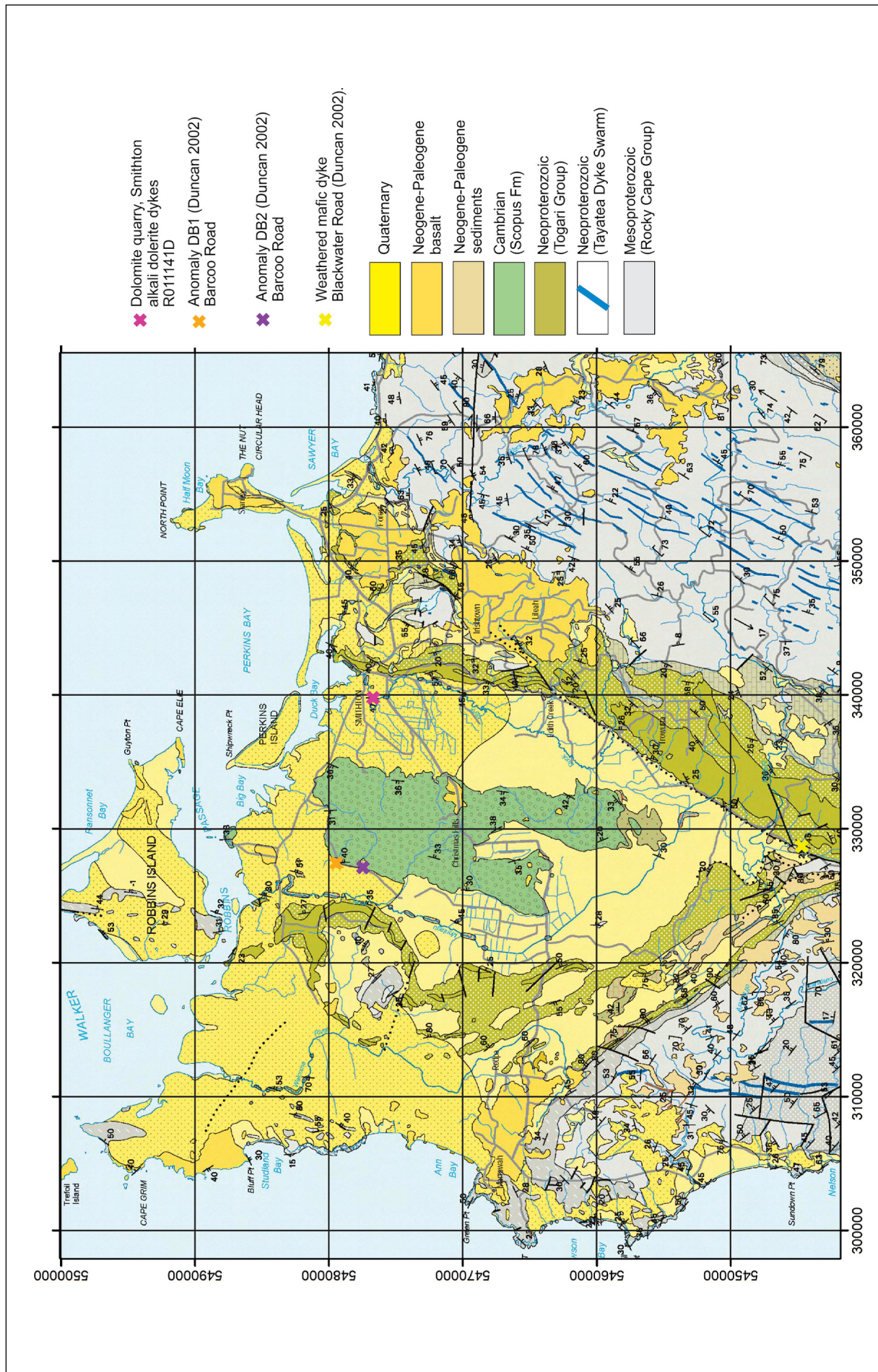


Figure 2. Generalised geology of far northwest Tasmania, derived from MRT 1:250,000 digital data.

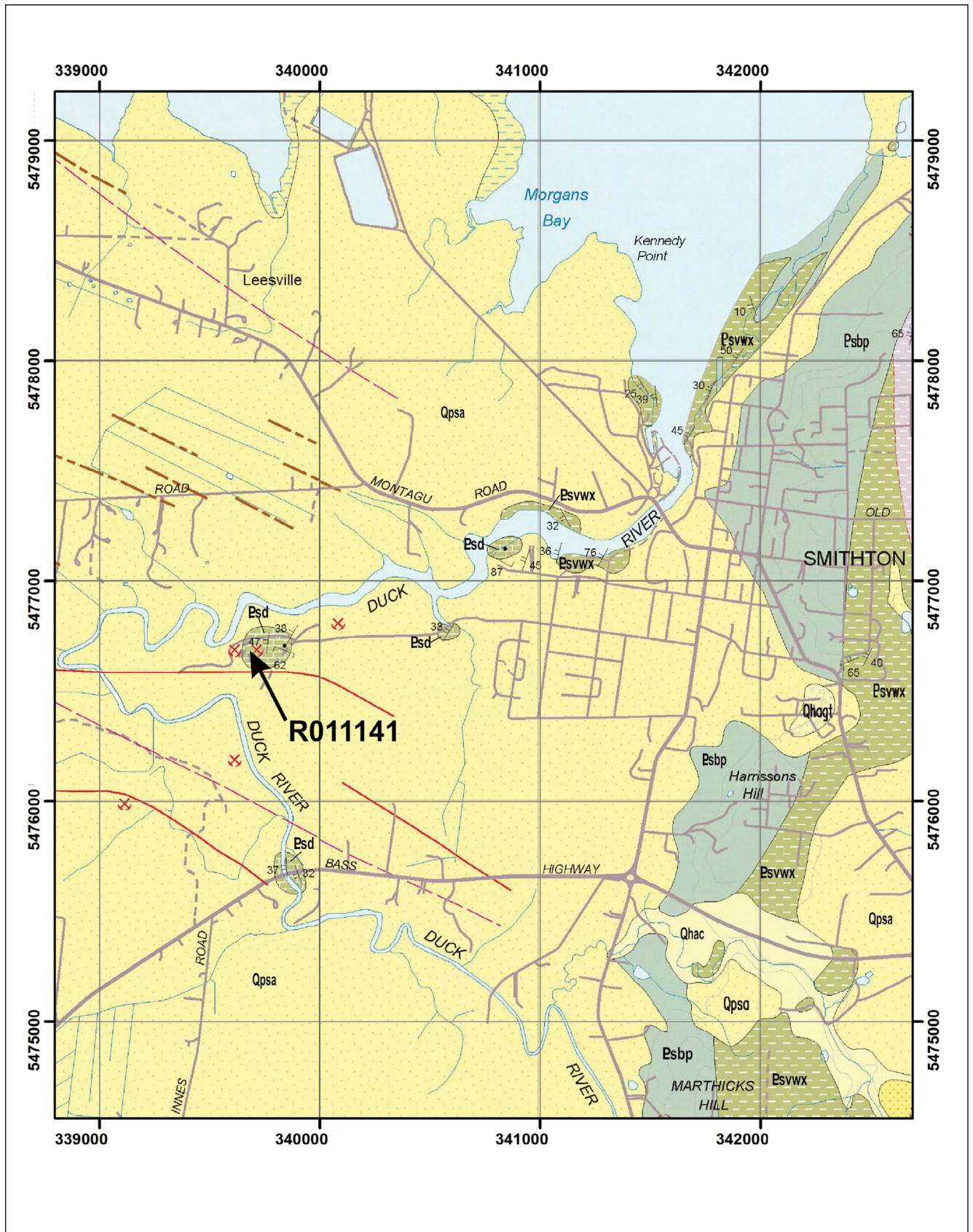


Figure 3. Detailed geology in vicinity of dolomite quarry, Smithton, derived from MRT 1:25,000 digital data (Seymour 2001, 2002). Neoproterozoic Toga Group units: Psd- Smithton Dolomite, Psvwx- Keppel Creek Formation (lithicwacke, siltstone and mudstone), Psbp- Spinks Creek Volcanics (basalt); Qpsa- aeolian sand. Sample location also shown.

Solid red lines - lineaments visible in airborne magnetic data;

Dashed purple line - lineament visible in airborne radiometric data;

Dashed brown lines - trend of relict beach ridges related to regressive strandlines of Last Interglacial Stage.



Figure 4. Dolerite dykes in dolomite quarry, Smithton, in 2001 (Photo - D. Duncan).



Figure 5. Dolerite dykes in dolomite quarry, Smithton, in 2006 (Photo - R. S. Bottrill).



Figure 6. Detail of dolerite dykes in dolomite quarry, Smithton, in 2014 (Photo - G. V. Cumming).

Duncan (2002) also identified a very weathered mafic dyke, with well-preserved igneous textures, intruding the Keppel Creek Formation in a cutting on Blackwater Road, ~25 km SSW of Smithton (328644 mE, 5444473 mN). The locality is also coincident with another WNW magnetic linear which extends for ~36 km between the Julius River and Arthur River estuary areas (Figure 1, 2). Relatively fresh outcrops of alkali dolerite were identified in the latter area, in and around Sky Creek (Cumming et al., 2017). J. Mulder (pers. comm.) obtained a ~540 Ma U-Pb age on apatite from a sample from Sky Creek, so these probably represent a different suite.

3.0 PETROGRAPHY

The Smithton quarry sample selected for geochronology (R011141D) consists of scattered, partly altered olivine phenocrysts in a dominantly subophitic groundmass of titaniferous augite, plagioclase, titanomagnetite and partly altered mesostasis, with amygdales of carbonate and/or smectite (Figures 7 and 8).

The olivine phenocrysts are generally \pm equant, ≤ 1.5 mm across, and partly (~20%) to completely altered to a fibrous, pleochroic (pale to medium yellow-brown), strongly birefringent, length-slow alteration product, probably an amphibole and possibly anthophyllite.

The bulk of the rock consists of a subophitic groundmass of pink-mauve titaniferous augite prisms (typically 500 μm -1mm long and 100-200 μm wide) and plagioclase laths (up to 600 x 100 μm). Equant angular opaque grains, mostly 20 – 50 μm across are fairly

abundant and are probably titanomagnetite/ulvospinel (see below). There is some interstitial, strongly zoned but apparently untwinned feldspar (possibly alkali feldspar) and pale yellow-brown alteration (probably smectite).

Numerous, round (mostly 0.5 – 1.5 mm diameter) to slightly flattened or irregular amygdales are filled with sparry carbonate and/or fine-grained pale brown smectite. In those amygdales in which both minerals are present, smectite forms the lining and carbonate the core (Figure 8).

The other fourteen thin sections are very similar, differing mainly in the degree of alteration, although all contain at least some relict unaltered olivine. One (DD1) contains a very well-rounded xenocrystic quartz grain, ~800 μm in diameter, surrounded by a narrow (~40 μm) reaction rim of radiating prisms of augite.

4.0 MINERAL CHEMISTRY

Bottrill (2004, Appendix 3) reported electron microprobe analyses of minerals from sample R011141. Clinopyroxene (two similar analyses) is subsilicic aluminian diopside in the classification of Morimoto (1988), with high Al_2O_3 (7.07, 7.25%) and TiO_2 (3.23, 3.47%). Plagioclase (two analyses) is labradorite ($\text{An}_{66.3-67.4}$). Analyses of ulvospinel (TiO_2 19.6 – 21.0%), saponite and siderite were also reported.

Visual examination and X-ray diffraction of three samples of dolostone, collected from level 1 of the quarry adjacent to the dykes, showed that all were pure dolomite, with no indication of any metamorphic or metasomatic reactions at the contacts (Renaud and Bottrill, 2022).

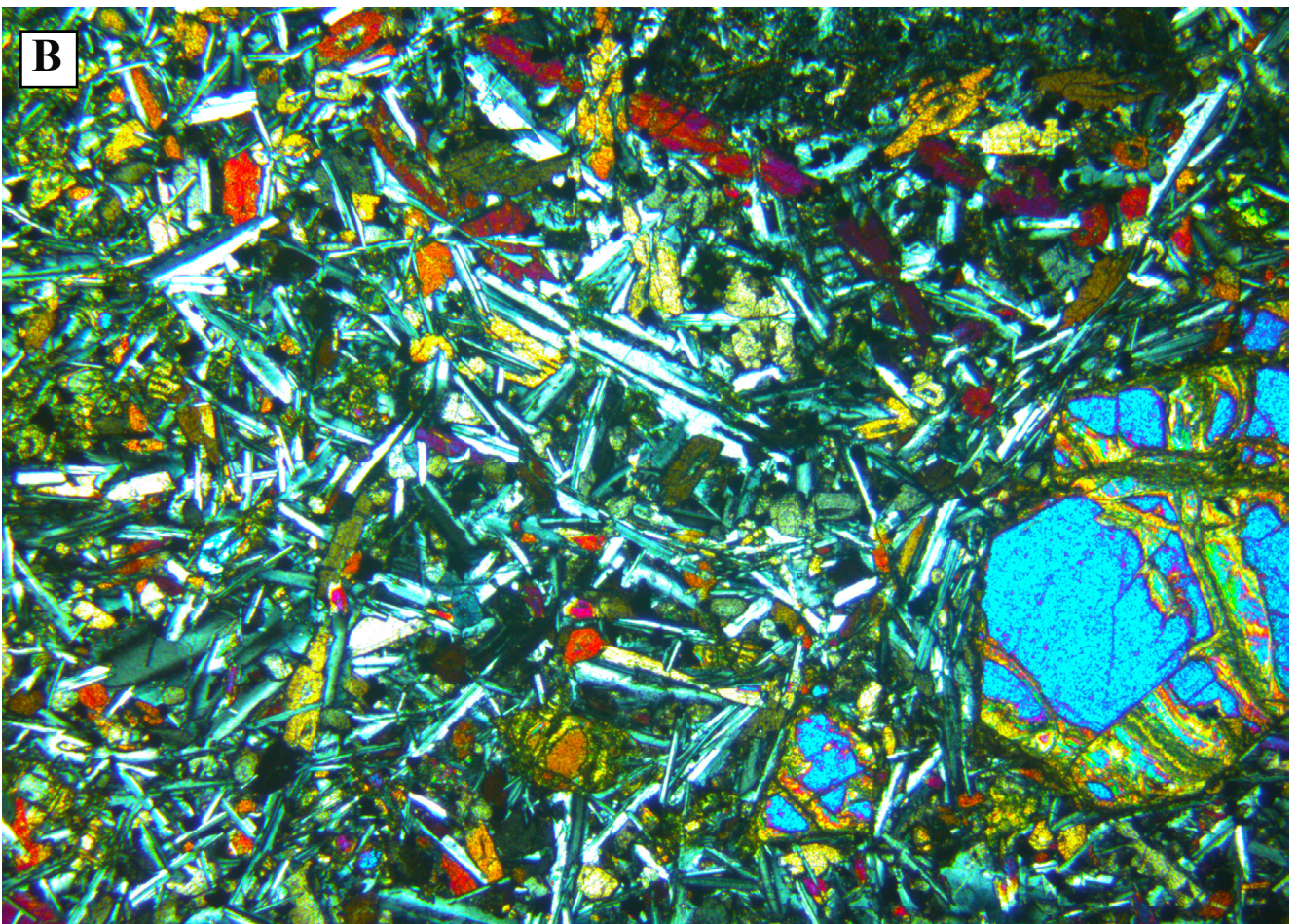
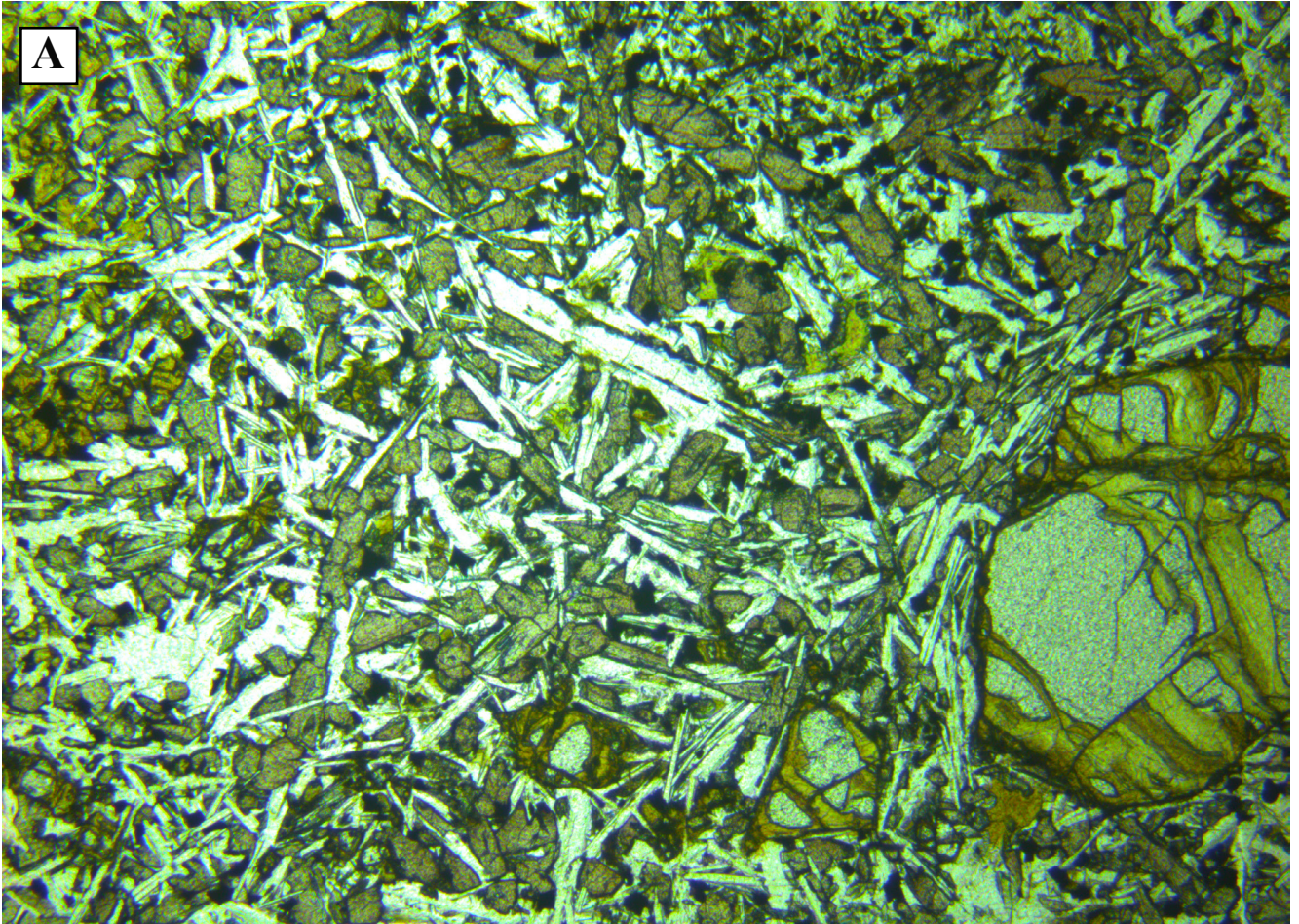


Figure 7. Photomicrograph of alkali dolerite sample R011141D, dolomite quarry, Smithton. Note partly altered olivine phenocryst (lower right), plagioclase laths (white), titaniferous augite (mauve). Field of view ~4.6 mm x 3.4 mm. A) plane polarised light, B) crossed nicols.

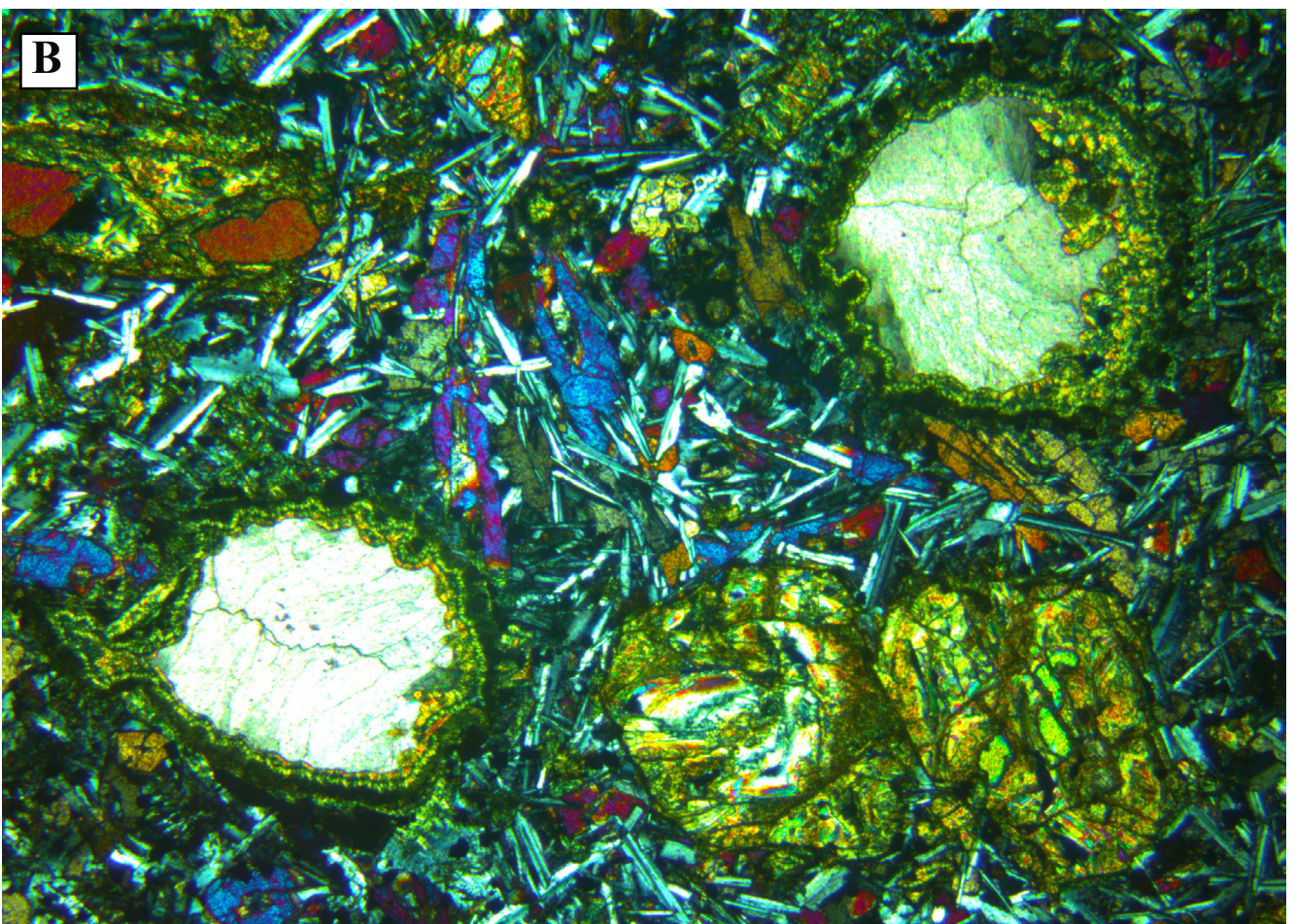
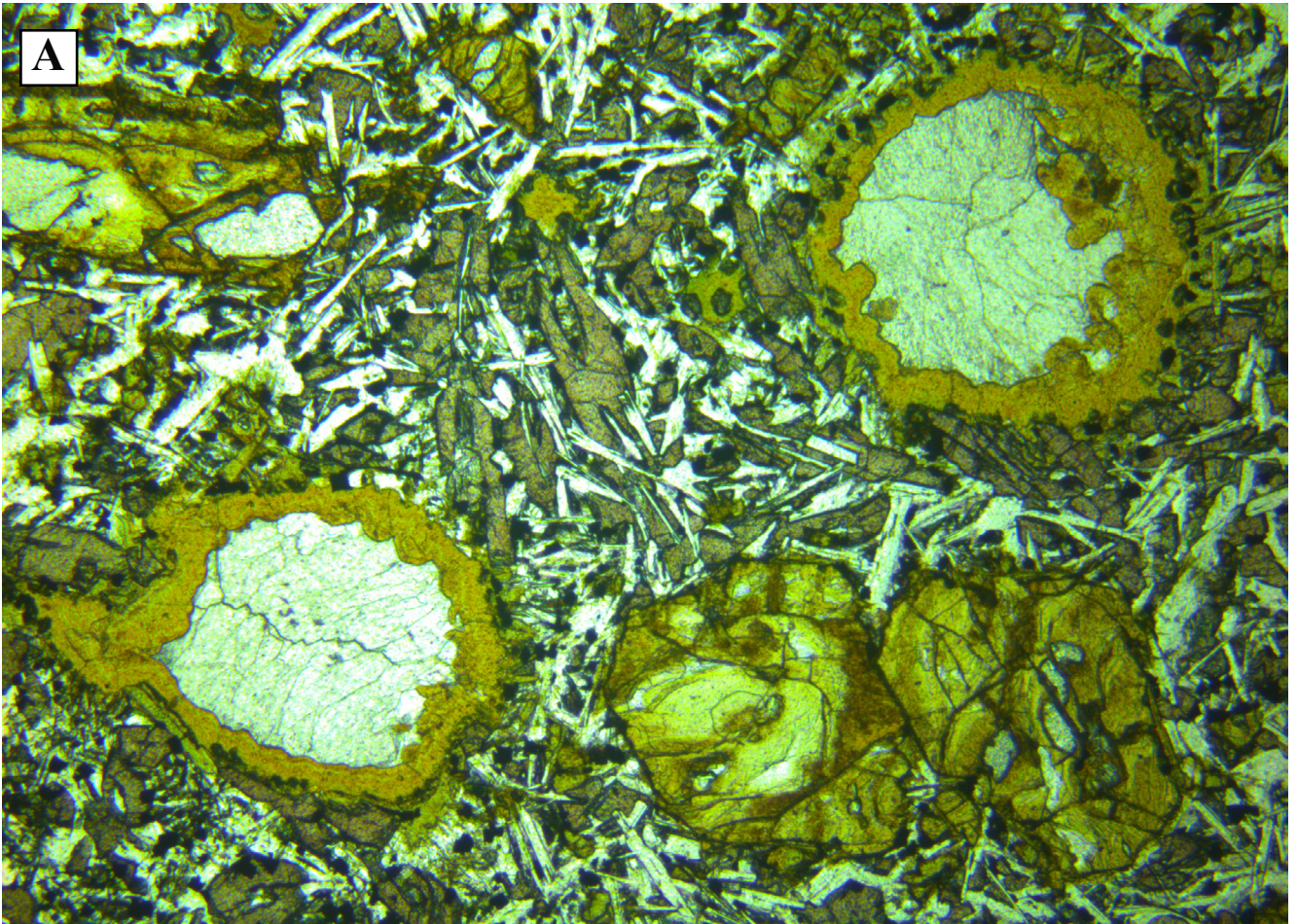


Figure 8. Photomicrograph of alkali dolerite sample R011141D, dolomite quarry, Smithton. Note altered olivine phenocrysts (lower right and upper left), amygdales (lower left and upper right) lined with smectite (brown) and filled with carbonate (white). Field of view ~4.6 mm x 3.4 mm. A) plane polarised light, B) crossed nicols.

5.0 GEOCHEMISTRY

Part of sample R0111141D was analysed in the MRT laboratories for major and trace elements by X-ray fluorescence (XRF), using standard techniques. Trace elements were also determined in some of the remaining powder by inductively coupled plasma mass spectroscopy (ICPMS) at the University of Melbourne. Results are in good agreement with XRF values (Appendix 1, Table 1).

The analysis contains 1.20% CO₂ and 3.26% H₂O+, consistent with secondary carbonate and clay minerals observed petrographically, but otherwise may be a near-magmatic composition. In the Johnson and Duggan (1989) normative classification, developed for Eastern Australian Cainozoic volcanics, it is a transitional olivine basalt (*ol* present, $0 < hy < 10\%$ in the

CIPW norm). In the IUGS total alkali-silica classification for volcanic rocks (Le Maitre 2002), it plots simply as basalt, in the field of overlap between alkalic and sub-alkalic fields. However, trace elements levels and ratios (e.g. Nb/Y >1) clearly indicate alkalic affinities, consistent with the presence of titaniferous augite. Low MgO and Mg# (58.5, also calculated at Fe₂O₃/FeO = 0.20) indicate a moderately fractionated composition.

The rock plots within the field of Tasmanian Cainozoic basalts for virtually all major and trace elements, although Al₂O₃ and CaO are slightly high, and TiO₂ slightly low, relative to Cainozoic basalts with similar SiO₂ and Mg# (Figure 9). The compatible trace elements Cr (382 ppm) and Ni (220 ppm) are also high, relative to Cainozoic basalts with similar Mg# (Figure 10).

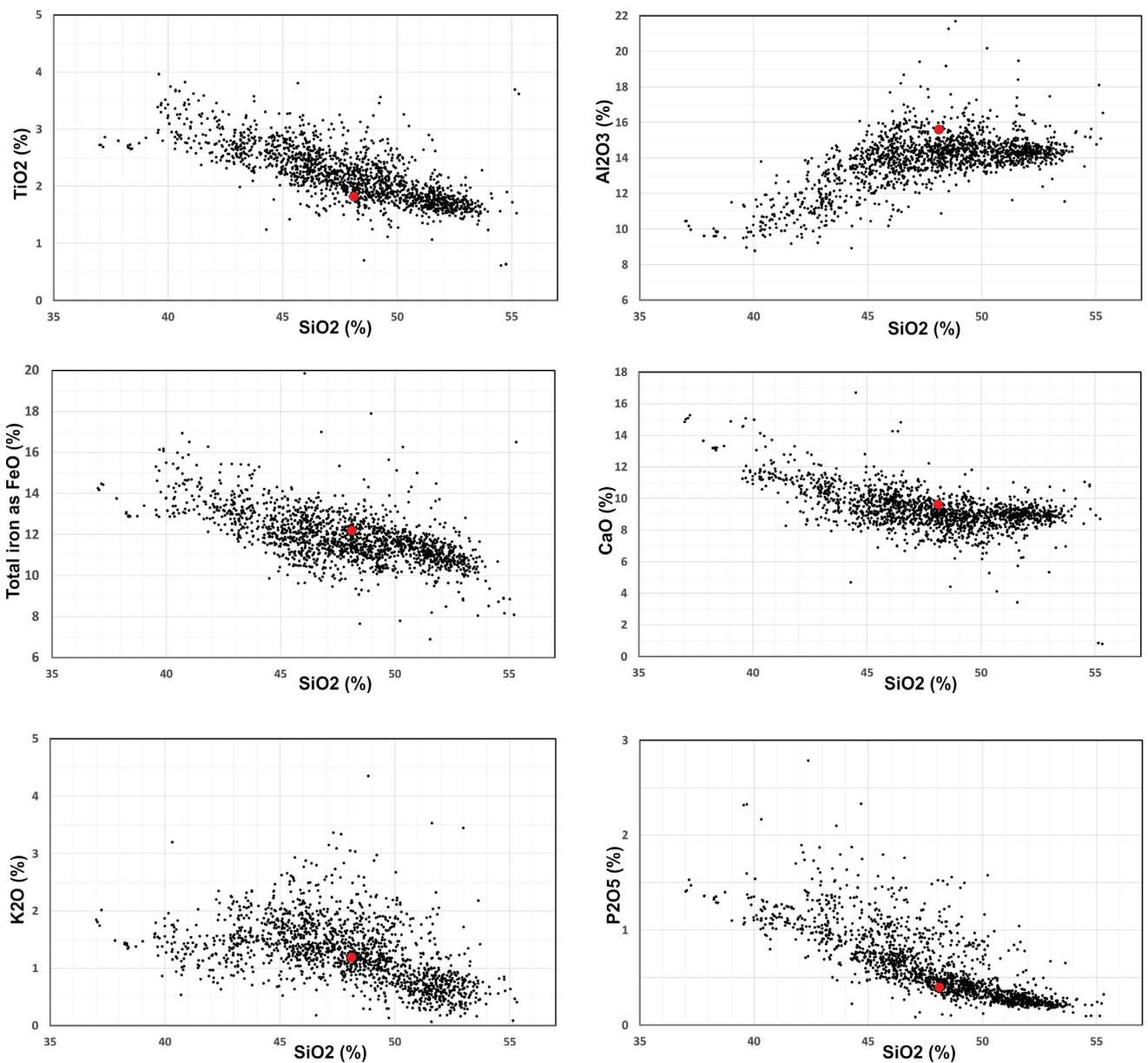


Figure 9. Plots of selected major elements for Smithton alkali dolerite (R011141D)(red circle), compared to Tasmanian Cainozoic basalts (block dots). Analyses normalised to 100% anhydrous, CO₂-free. (a) TiO₂ vs. SiO₂ (b) Al₂O₃ vs SiO₂ (c) total iron as FeO vs SiO₂ (d) CaO vs. SiO₂ (e] K₂O vs. SiO₂ (f) P₂O₅ vs. SiO₂.

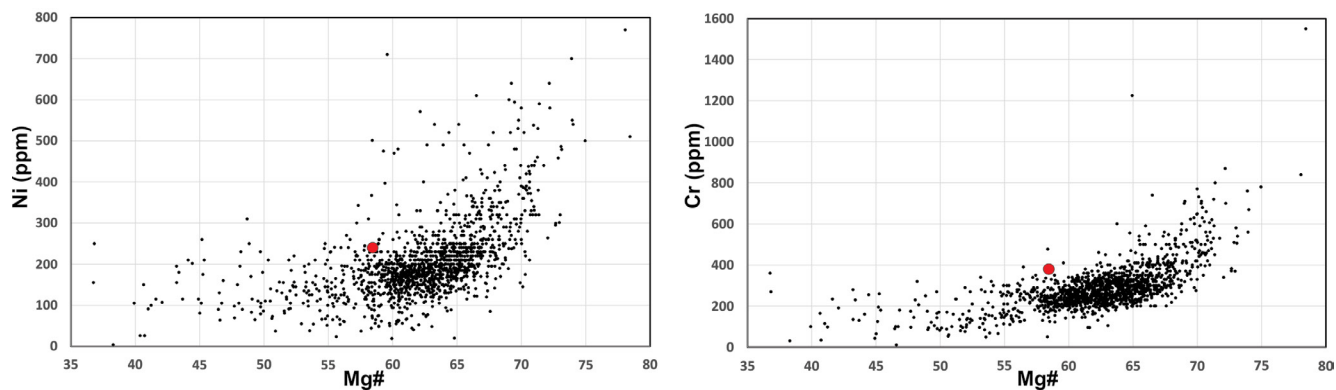


Figure 10. Plots of compatible trace elements for Smithton alkali dolerite (R011141D)(red circle), compared to Tasmanian Cainozoic basalts (block dots). (a) Ni vs Mg# (b) Cr vs. Mg#; Mg# is molar $100\text{Mg}/(\text{Mg} + \text{Fe}^{\text{II}})$ calculated as $\text{Fe}_2\text{O}_3/\text{FeO} = 0.20$.

The chondrite-normalised rare earth element (REE) pattern of R011141D is moderately light rare earth element (LREE) enriched ($(\text{La}/\text{Yb})_{\text{N}} = 7.84$), slight concave, with $\text{La}_{\text{N}} \sim 85.8$, $\text{Yb}_{\text{N}} \sim 10.9$ and no Eu anomaly (Figure 11). It resembles that of Cainozoic basalts of similar major element composition, from northwest Tasmania and elsewhere.

Incompatible elements, when normalised to model Primitive Mantle and plotted in order of decreasing mantle incompatibility (Sun and McDonough, 1989), produce a nearly smooth pattern, apart from a small positive Pb anomaly, with a moderate peak at Nb and Ta. A more jagged pattern displayed by the very incompatible elements Cs, Rb and Ba may be due to alteration, as these elements are also commonly mobile (e.g. Rollinson 1993).

In northwest Tasmania, broadly similar patterns are displayed by Cainozoic basalts of similar composition, e.g. TJ3591 (34 Ma transitional olivine basalt, Rabalga Track); TJ3602 (27 Ma hawaiite, Wedge Plains Link Road) (Everard et al., 2014; Figure 12). However, these have a less pronounced peak at Nb-Ta-(K), and larger Pb anomalies.

Zhang et al. (2014) reported three types of mantle-normalised trace elements patterns in Tasmanian Cainozoic basalts. The smooth pattern displayed by R011141D, with a moderate peak at Nb and Ta, is typical of “alkali olivine basalts, many hawaiites and transitional olivine basalts, some basanites and a few nepheline hawaiites.” It contrasts with patterns with strong positive Pb, U and K displayed by tholeiites, and patterns with “strong depletions in K and usually Rb, and moderately weak depletions in Zr, Hf and Ta” seen in strongly undersaturated basanites and nephelinites. It is also unlike the jagged pattern displayed by Jurassic dolerite (e.g. Hergt et al., 1989).

Bottrill et al. (2014) briefly reported initial isotopic ratios for sample R011141D, corrected to 96 Ma, of $^{87}\text{Sr}/^{86}\text{Sr} = 0.70380$ and $^{143}\text{Nd}/^{144}\text{Nd} = 0.512741$ ($\epsilon\text{Nd} = +4.41$). Full

analytical details are given in Table 2. These values are also within the range displayed by similar Tasmanian Cainozoic basalts.

6.0 GEOCHRONOLOGY

A feldspar concentrate (20 g) was separated from sample R011141d. Preparation, irradiation, step-heating, analysis and data reduction followed a procedure similar to that described in Everard et al. (2004). A detailed account of the ^{40}Ar - ^{39}Ar dating technique (McDougall and Harrison, 1999) underpins the dating presented here.

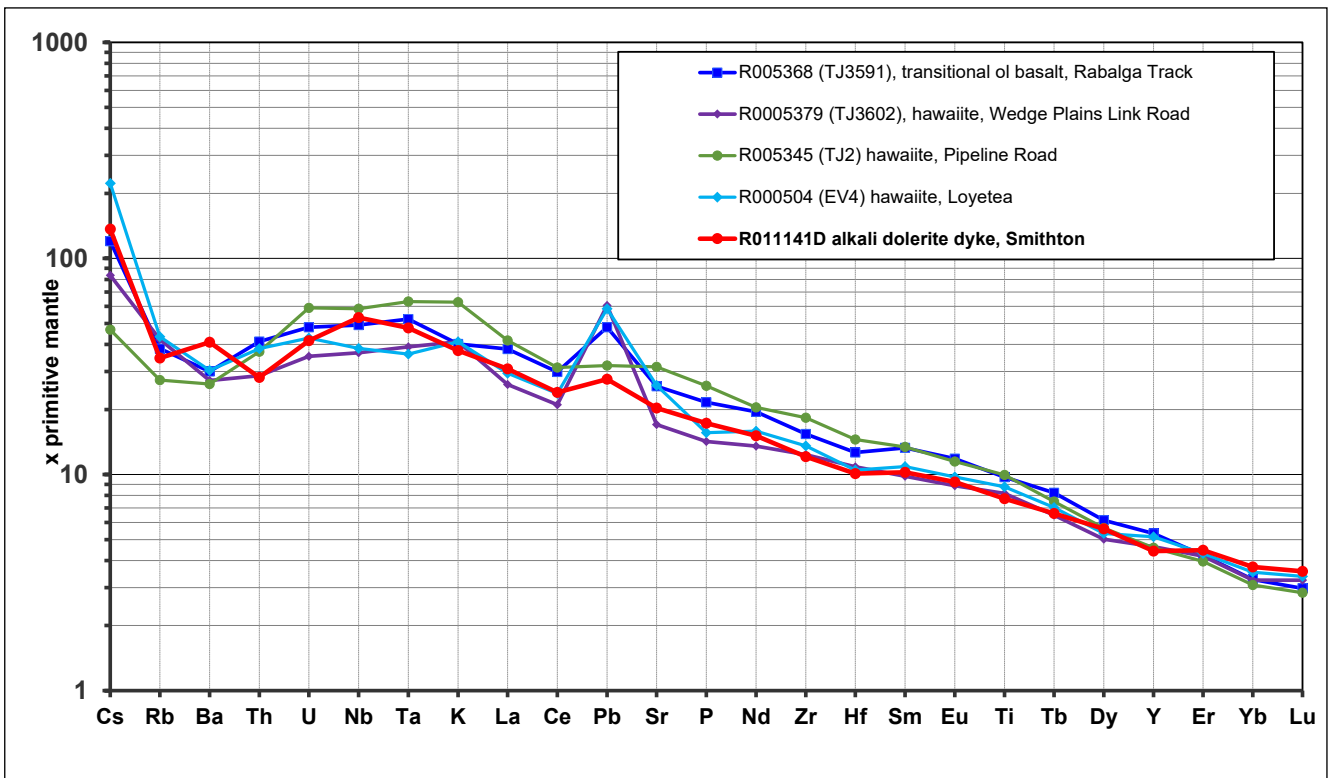
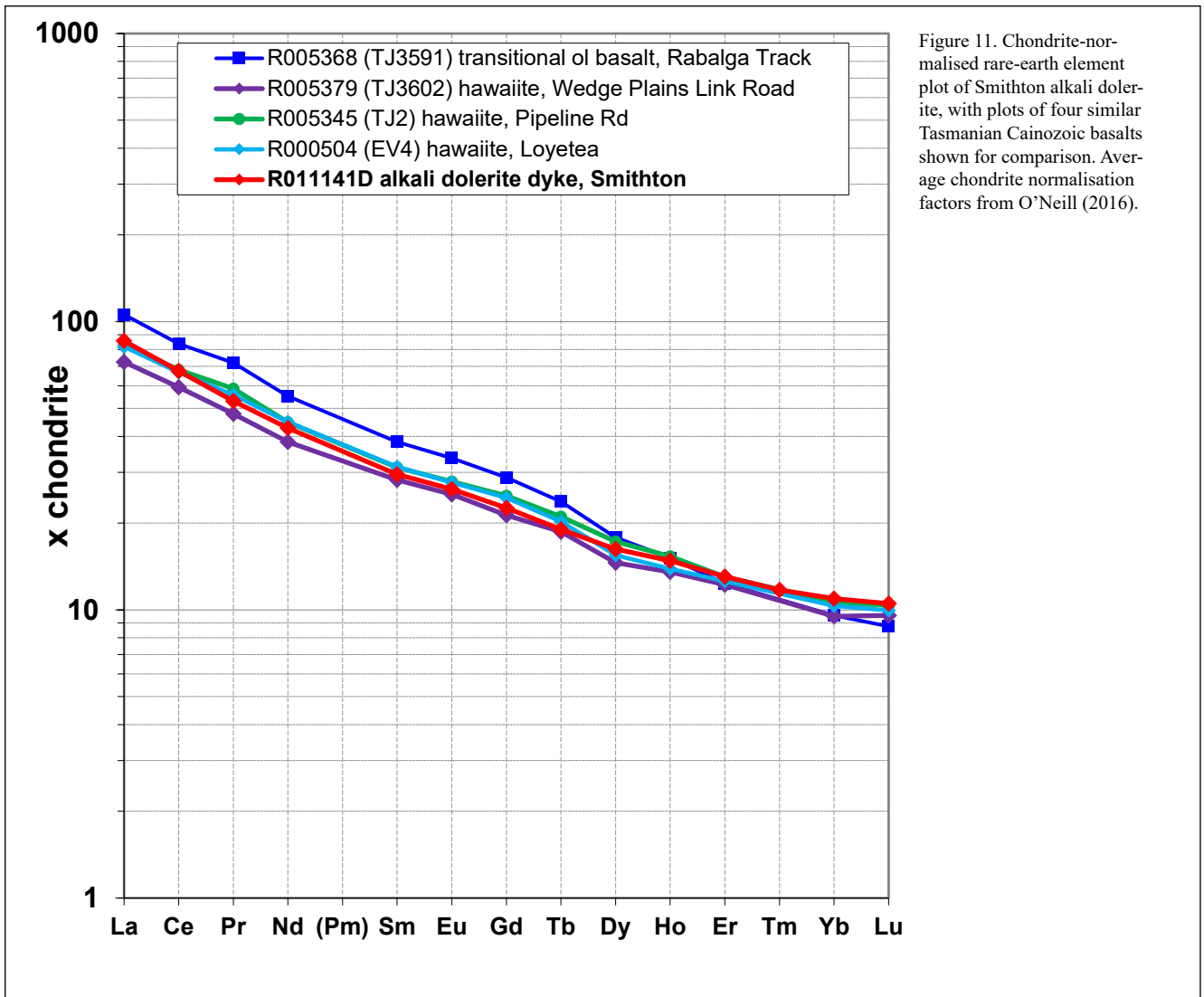
Ar-Ar ages were calculated using decay constants of Steiger and Jäger (1977). Weighted mean ages were calculated ($\pm 2\sigma$ errors) using the Ludwig (2001) Isoplot program.

The apparent ages of ten heating steps range from 111.96 Ma (step 1) to 86.31 Ma (step 9) and do not define a plateau (Appendix 1, Table 3; Figure 13). The total gas age, analogous to a $^{40}\text{K}/^{40}\text{Ar}$ age, of 95.93 ± 7.37 Ma is, however, considered to be the best estimate of the crystallisation age. The inverse isochron ($^{36}\text{Ar}/^{40}\text{Ar}$ vs $^{39}\text{Ar}/^{40}\text{Ar}$) age of 101 ± 19 Ma (Figure 14) is within error of the total gas age.

7.0 DISCUSSION AND CONCLUSION

Although imprecise, these data strongly suggest a mid-Cretaceous age (probably early Late Cretaceous) for these dykes of alkali dolerite. On the most recent IGC time scale (Cohen, 2022), 95.9 Ma is Cenomanian, with the range (± 7.37 Myr) also including the Turonian, early Coniacian and latest Albian.

Igneous rocks of Cretaceous age are rare in Tasmania, the major examples being the Cygnet Alkaline Complex in southeast Tasmania (~ 100 Ma; Evernden and Richards, 1962; McDougall and Leggo, 1965) in southeast Tasmania and the Cape Portland shoshonite complex and related rocks in northeast Tasmania (102.3 ± 2.6 , McDougall and Green, 1982; 98.7 ± 0.6 Ma, Baillie, 1986). Also in northeast Tasmania, the



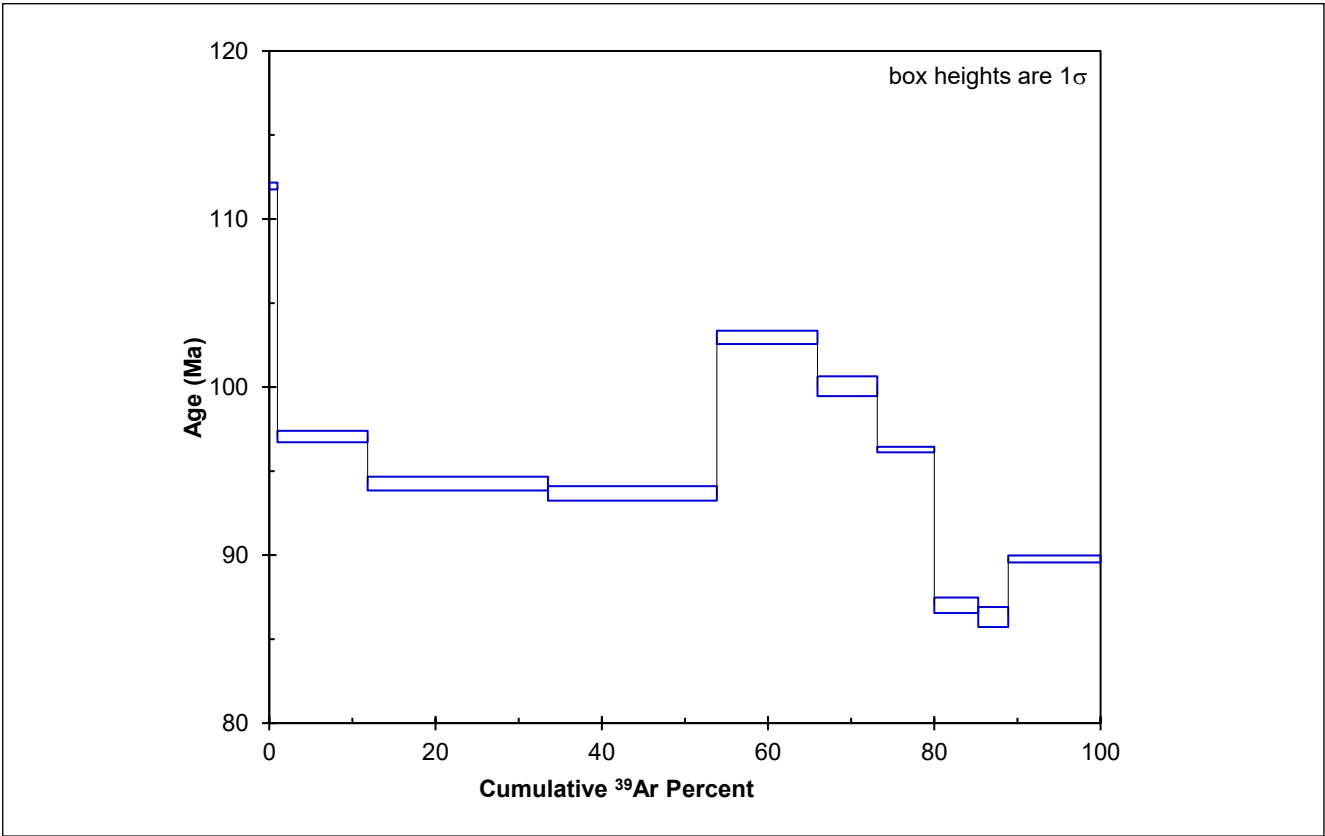


Figure 13. ^{39}Ar -age degassing spectrum.

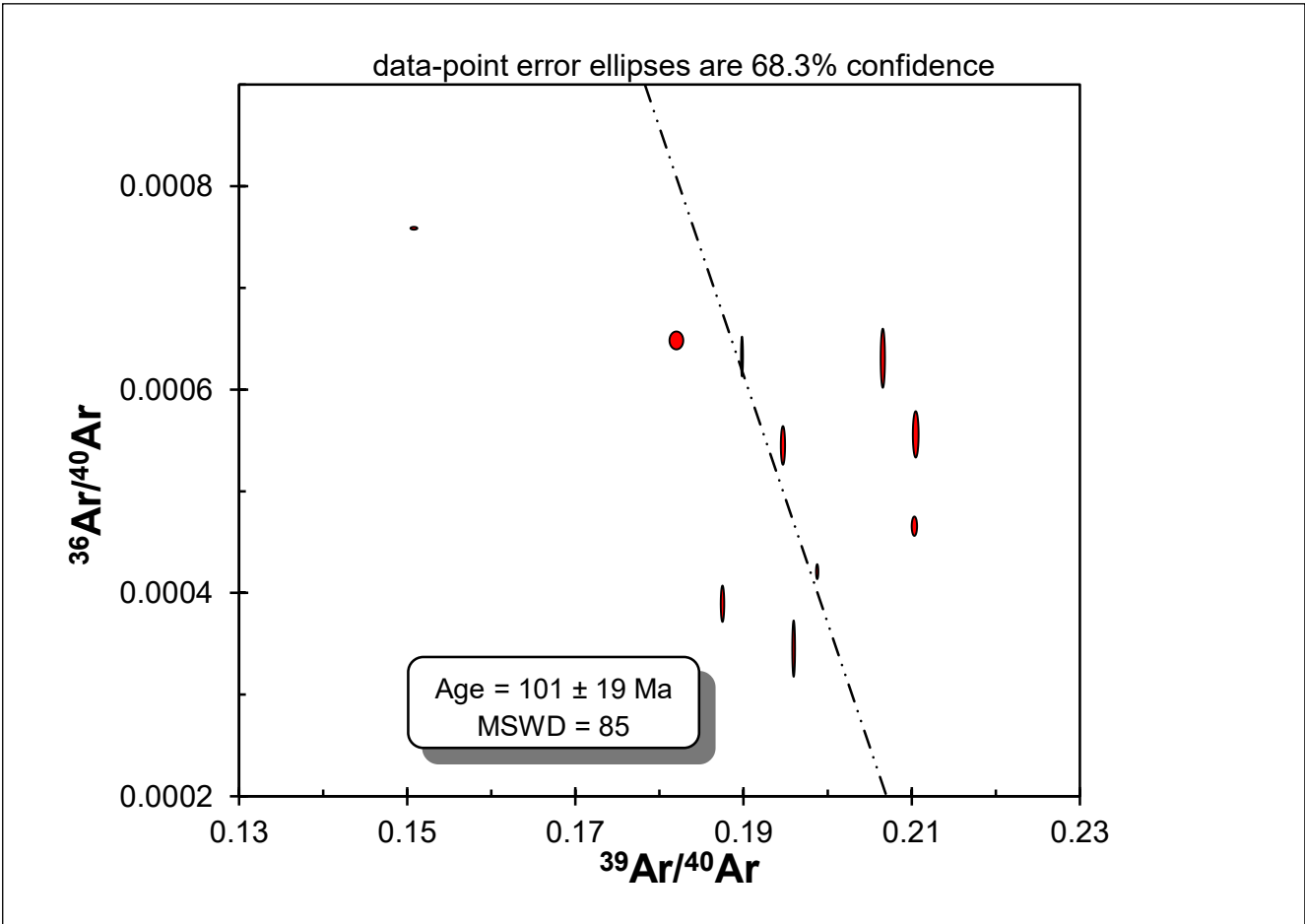


Figure 14. Inverse isochron, $^{36}\text{Ar}/^{40}\text{Ar}$ vs $^{39}\text{Ar}/^{40}\text{Ar}$.

Tomahawk River phonolite was dated at ~80 Ma (K/Ar) and ~76 Ma ($^{40}\text{Ar}/^{39}\text{Ar}$) (Everard et al., 2004). A lamprophyre dyke from the east coast of King Island was dated at 140 Ma (K/Ar, McDougall and Leggo, 1965). All these rocks are petrologically unlike the alkali dolerite dykes at Smithton, and are spatially far removed from them.

However, the dykes are virtually indistinguishable from certain Tasmanian Cainozoic basalts in their petrography, major and trace element geochemistry and Sr and Nd isotopic ratios. Despite the difference in age, it is likely that they were derived by partial melting of the same mantle source or sources that later produced the more voluminous Cainozoic magmatism. For these mildly alkalic compositions, this may have been Pacific MORB-type source, possibly with a HIMU-component derived from the head of the Balleny plume which passed near Tasmania at 90-100 Ma (Zhang et al., 2014; Crawford et al., 1997).

Their age, although imprecise, is approximately coeval with the end of the Otway Rift Phase, the earliest stage in the development of Bass Basin. This was accompanied by NNE-directed tension and the development of WNW-trending normal faults, consistent with the orientation of the dykes (Baillie and Quilty, 2014). It was followed by the commencement of rifting between Australia-New Zealand and Antarctica at 96 Ma (e.g. Muller et al., 2000).

7.0 ACKNOWLEDGEMENTS

MRT technical staff are thanked for assistance with analytical work. G. V. Cumming supplied Figure 6. A. J. Crawford arranged ICPMS and isotope analyses at the University of Melbourne. F. L. Sutherland advised on the suitability of the sample for dating. C. Large prepared the manuscript for publication.

8.0 REFERENCES

- Baillie, P. W. 1986. Geological Survey Explanatory Report. Sheet 8516S (25). *Eddystone*. Tasmania Department of Mines.
- Baillie, P. W. and Quilty, P. G. 2014. Bass Basin. In: Corbett K. D., Quilty P. G. and Calver C. R. (eds.). Geological Evolution of Tasmania. *Geological Society of Australia Special Publication*, 24, 429-437.
- Bottrill, R. S. 2004. Petrology and geochemistry of some rock samples collected for the WTRMP Project, northwestern Tasmania. *Tasmanian Geological Survey Record* 2004/07.
- Bottrill, R. S., Everard, J. L. and Taheri, J. 2014. Cretaceous igneous rocks. in: Corbett K. D., Quilty P. G. and Calver C. R. (eds.). Geological Evolution of Tasmania. *Geological Society of Australia Special Publication*, 24, 453-463.
- Crawford, A. J., Lanyon, R., Elmes, M. and Eggins, S. 1997. Geochemistry and significance of basaltic rocks dredged from the South Tasman Rise and adjacent seamounts. *Australian Journal of Earth Sciences*, 44, 621-632.
- Cumming, G. V., Everard, J. L. and Calver, C. R. 2017. Digital geological atlas 1:25,000 scale series. Sheet 3045. *Bluff*. Mineral Resources Tasmania.
- Duncan, D. McP. 2002. Western Tasmanian Regional Minerals Program- Area 3, northwest Tasmania. *Tasmanian Geological Survey Record* 2002/21.
- Everard, J. L., Sutherland, F. L. and Zwingmann, H. 2004. A Cretaceous phonolite dyke from the Tomahawk River, northeast Tasmania. *Papers and Proceedings of the Royal Society of Tasmania*, 138, 11-33.
- Everard, J. L., Bailie, P. W., Beyer, E. E. Doyle, R. B. O'Reilly, S. Y and Zhang, M. 2014. Palaeogene-Neogene basaltic volcanism. In: Corbett K. D., Quilty P. G. and Calver C.R. (eds.). The Geological Evolution of Tasmania. *Geological Society of Australia Special Publication*, 24, 463 – 494.
- Evernden, J. F. and Richards, J. R. 1962. Potassium-argon ages in eastern Australia. *Journal of the Geological Society of Australia*, 9, 1–49.
- Hergt, J. M., Chappell, B. W., McCulloch, M. T., McDougall, I. and Chivas, A. R. 1989. Geochemical and isotopic constraints on the origin of the Jurassic dolerites of Tasmania. *Journal of Petrology*, 30, 841-833.
- Hess, J. C. and Lippolt, H. J. 1994. Compilation of K-Ar measurements on HD-B1 standard biotite 1994 status report. Phanerozoic Time Scale. G. S. Odin, Paris. *Bulletin of Liaison and Information*, IUGS Subcommittee of Geochronology 12: 19-23.
- Johnson, R. W. and Duggan, M. B. 1989. Rock classification and analytical data bases. In: Johnson, R. W. (ed.). *Intraplate Volcanism in Eastern Australia and New Zealand*, 2-13. Cambridge University Press.
- Le Maitre, R.W. (ed.) 2002. *A Classification of Igneous Rocks and Glossary of Terms*, 2nd Edition. Cambridge University Press, 236.
- Lennox, P. G., Corbett, K. D., Baillie, P. W., Corbett, E. B. and Brown, A. V. 1982. Geological Atlas 1:50,000 Series, Sheet 21 (7916S). *Smithton*. Department of Mines Tasmania.
- Ludwig, K. R. 2001. Isoplot/Ex rev. 2.49, a Geochronological Toolkit for Microsoft Excel. *Berkeley Geochronology Centre Special Publication*, 1a.
- McDougall, I. and Harrison, T. M. 1999. *Geochronology and Thermochronology by the ⁴⁰Ar/³⁹Ar method*, 2nd Edition. Oxford University Press, New York, 269.
- McDougall, I. and Leggo, P. J. 1965. Isotopic age determinations on granitic rocks from Tasmania. *Journal of the Geological Society of Australia*, 12, 295–332.
- McDougall, I. and Green, D. C. 1982. Cretaceous K/Ar ages from north-eastern Tasmania. Appendix 3 in McClenaghan M.P., Turner N.J., Baillie P.W., Brown A.V., Williams P.R. and Moore W. R. 1982. Geology of the Ringarooma- Boobyalla area. *Geological Survey of Tasmania Bulletin*, 61.
- Morimoto, N. 1988. Nomenclature of pyroxenes. *American Mineralogist*, 73, 1123-1133.
- O'Neill, H. St. C. 2016. The smoothness and shapes of chondrite-normalized rare earth element patterns in basalts. *Journal of Petrology*, 57, 1463-1508.
- Muller, R. D., Gaina, C. and Clark S. 2000. Seafloor spreading around Australia. in: Veevers J. (ed.) *Billion-year earth history of Australia and its neighbours in Gondwanaland*. GEMOC Press, Sydney, 18-27.

- Pemberton, J. 1983. *Annual report EL25/80, Montagu, 1982 season*. Geopeko Ltd. [TCR83-1950].
- Renaud, J. and Bottrill R. S. 2022. Mineralogical examination of dolomite samples, Smithton. Mineral Resources Tasmania Laboratory Report LJN2022-101 (unpublished).
- Rollinson, H. R. 1993. *Using Geochemical Data: Evaluation, Presentation, Interpretation*. Longman.
- Seymour, D. B. 2001. Digital geological atlas 1:25,000 scale series. Sheet 3247. *Mella*. Mineral Resources Tasmania.
- Seymour, D. B. 2002. Digital geological atlas 1:25,000 scale series. Sheet 3447. *Smithton*. Mineral Resources Tasmania.
- Steiger, R. H. and Jäger, E. 1977. Subcommittee on Geochronology: convention on the use of decay constants in geo- and cosmochemistry. *Earth and Planetary Science Letters*, 36, 359-362.
- Sun, S.-S. and McDonough W. F. 1989. Chemical and isotopic systematics of oceanic basalts: implications for mantle composition and processes. In: Saunders, A. D. and Norry, M. J. (eds.) *Magma-tism in the Ocean Basins. Geological Society of London Special Publication*, 42, 313-346.
- Zhang M., O'Reilly, S. Y. and Everard J. L. 2014. Mantle sources and petrogenesis. In: Corbett K. D., Quilty P. G. and Calver C.R. (eds.) 2014. *The Geological Evolution of Tasmania. Geological Society of Australia Special Publication*, 24, 485 – 486.

APPENDIX 1

Tables of analytical data

Table 1. Whole rock geochemistry, sample R011141D

Major elements (%)		Trace Elements (ppm)		
	<i>XRF</i>		<i>ICPMS</i>	<i>XRF</i>
SiO₂	45.66	Li	10.1	
TiO₂	1.73	Be	1.2	
Al₂O₃	14.80	Ca	66091	[65252]
Fe₂O₃	3.62	Sc	20.6	25
FeO	8.31	Ti	10042	[10400]
MnO	0.15	V	195	170
MgO	7.74	Cr	382	380
CaO	9.13	Co	51	53
Na₂O	2.62	Ni	220	240
K₂O	1.13	Cu	72	71
P₂O₅	0.38	Zn	88	100
SO₃	0.00	Ga	17.7	20
CO₂	1.20	As	0.6	<20
H₂O+	3.26	Rb	22.0	27
TOTAL	99.74	Sr	429	460
LOI	3.54	Y	20.1	23
FeOt	11.57	Zr	135	155
Mg#	58.45	Nb	38.0	43
(at Fe ₂ O ₃ /FeO = 0.20)		Mo	1.8	<5
		Cd	0.1	
CIPW norm		Sn	1.5	<9
(at Fe ₂ O ₃ /FeO = 0.20)		Sb	0.1	
<i>or</i>	7.01	Cs	1.1	
<i>ab</i>	23.34	Ba	286	320
<i>an</i>	26.56	La	21.20	<20
<i>di</i>	15.10	Ce	42.58	49
<i>hy</i>	2.24	Pr	5.04	
<i>ol</i>	18.38	Nd	20.47	<20
<i>mt</i>	2.99	Sm	4.55	
<i>il</i>	3.45	Eu	1.55	
<i>ap</i>	0.93	Gd	4.64	
<i>total</i>	100.00	Tb	0.71	
mol% An	51.75	Dy	4.13	
		Ho	0.82	
		Er	2.14	
		Tm	0.30	
		Yb	1.84	
		Lu	0.26	
		Hf	3.12	
		Ta	1.96	
		W	0.49	<10
		Tl	0.07	
		Pb	1.96	<10
		Bi		<5
		Th	2.39	<10
		U	0.87	<10

Table 2. Isotope data, sample R011141D

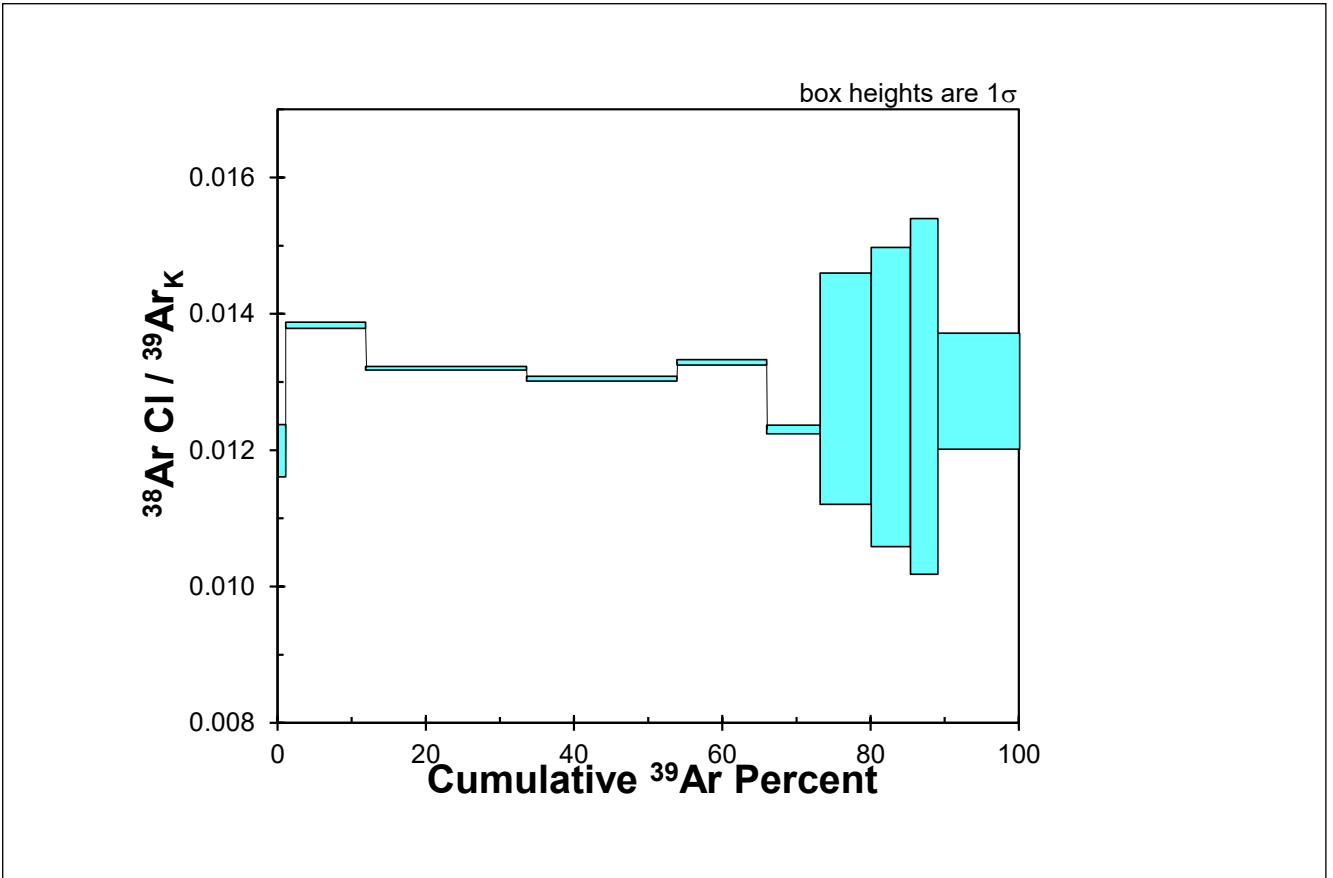
Rb (isotope dilution)	21	ppm
Sr (isotope dilution)	428	ppm
$^{87}\text{Rb}/^{86}\text{Sr}$	0.45	
$^{87}\text{Sr}/^{86}\text{Sr}$ (measured)	0.703996	(now)
$^{87}\text{Sr}/^{86}\text{Sr}$ (initial)	0.703798	at 96 Ma
Sm (ICPMS)	4.55	ppm
Nd (ICPMS)	428	ppm
$^{147}\text{Sm}/^{144}\text{Nd}$	0.1344	
$^{143}\text{Nd}/^{144}\text{Nd}$ (measured)	0.512825	(now)
ϵNd	3.65	(now)
$^{143}\text{Nd}/^{144}\text{Nd}$ (initial)	0.512741	at 96 Ma
ϵNd_i	4.41	at 96 Ma

Table 3. $^{40}\text{Ar}/^{39}\text{Ar}$ step heating analytical results for sample R011141D

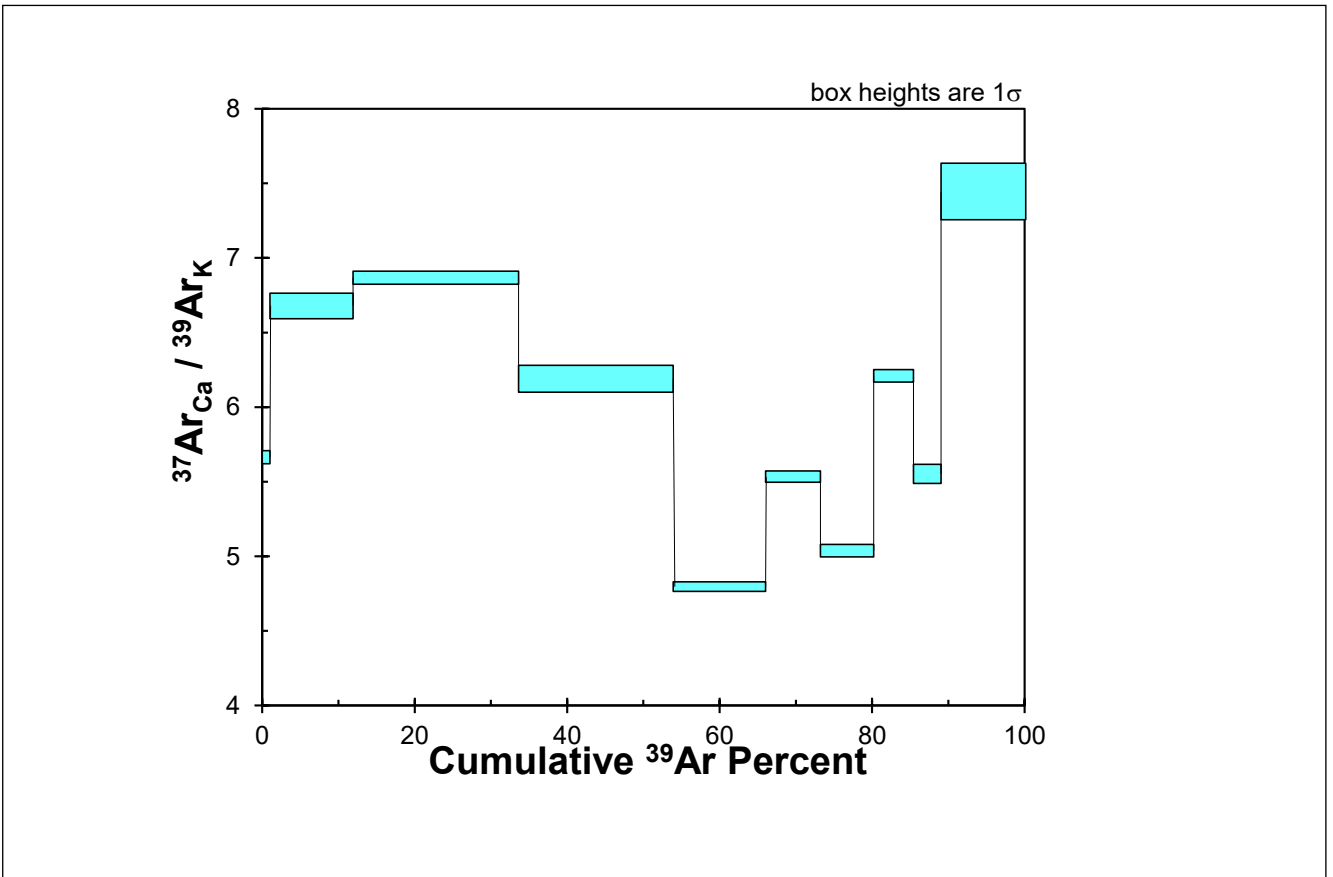
Type	Age (Ma)	+-	cumulative % ^{39}Ar	% atmos ^{40}Ar	CSIRO ID : 640 PLAGIOCLASE													
					$^{40}\text{Ar}^*/^{39}\text{Ar}$	+-	$^{40}\text{Ar}/^{39}\text{Ar}$	+-	$^{38}\text{Ar}/^{39}\text{Ar}$	+-	$^{37}\text{Ar}/^{39}\text{Ar}$	+-	$^{36}\text{Ar}/^{39}\text{Ar}$	+-	$^{39}\text{Ar}/^{40}\text{Ar}$	+-	$^{36}\text{Ar}/^{40}\text{Ar}$	+-
Step 1	111.96	0.58	0.99	22.45	5.1415	0.0097	6.6299	0.0107	0.0120	0.0004	5.6699	0.0411	0.0050	0.0000	0.1508	0.0002	0.0008	0.00000
Step 2	97.06	0.58	11.84	19.19	4.4383	0.0160	5.4926	0.0154	0.0138	0.0000	6.6862	0.0864	0.0036	0.0000	0.1821	0.0005	0.0006	0.00001
Step 3	94.25	0.61	33.53	16.15	4.3069	0.0192	5.1365	0.0039	0.0132	0.0000	6.8762	0.0442	0.0028	0.0001	0.1947	0.0001	0.0005	0.00001
Step 4	93.67	0.63	53.84	18.74	4.2795	0.0202	5.2661	0.0016	0.0131	0.0000	6.1977	0.0917	0.0033	0.0001	0.1899	0.0001	0.0006	0.00001
Step 5	102.96	0.64	65.95	11.55	4.7160	0.0187	5.3316	0.0037	0.0133	0.0000	4.8050	0.0282	0.0021	0.0001	0.1876	0.0001	0.0004	0.00001
Step 6	100.05	0.76	73.14	10.24	4.5791	0.0277	5.1016	0.0020	0.0123	0.0001	5.5432	0.0394	0.0018	0.0001	0.1960	0.0001	0.0003	0.00002
Step 7	96.28	0.49	80.00	12.47	4.4019	0.0077	5.0292	0.0029	0.0129	0.0017	5.0451	0.0406	0.0021	0.0000	0.1988	0.0001	0.0004	0.00000
Step 8	87.01	0.63	85.29	16.47	3.9679	0.0215	4.7500	0.0053	0.0128	0.0022	6.2198	0.0415	0.0026	0.0001	0.2105	0.0002	0.0006	0.00001
Step 9	86.31	0.73	88.89	18.68	3.9352	0.0278	4.8394	0.0038	0.0128	0.0026	5.5599	0.0622	0.0031	0.0001	0.2066	0.0002	0.0006	0.00002
Step 10	89.77	0.48	100.00	13.81	4.0968	0.0097	4.7529	0.0042	0.0129	0.0008	7.4523	0.1886	0.0022	0.0000	0.2104	0.0002	0.0005	0.00001
total gas age	95.93	7.37													Inverse isochron age 101 ± 19 Ma			

APPENDIX 2

Supplementary degassing spectra



$^{38}\text{Ar}_{\text{Cl}} / ^{39}\text{Ar}_{\text{K}}$ vs. cumulative ^{39}Ar % degassing spectrum.



$^{37}\text{Ar}_{\text{Ca}} / ^{39}\text{Ar}_{\text{K}}$ vs. cumulative ^{39}Ar % degassing spectrum.



Tasmanian
Government

Mineral Resources Tasmania

PO Box 56 Rosny Park

Tasmania Australia 7018

Ph: +61 3 6165 4800

info@mrt.tas.gov.au www.mrt.tas.gov.au